



Deep-ultraviolet transparent monolithic sol-gel derived silica-REPO₄ (RE = Y, La-Lu except Pm) glass-ceramics: characterization of crystal structure and ultraviolet absorption edge, and application to narrow-band UVB phosphors

Journal:	<i>Journal of Materials Chemistry C</i>
Manuscript ID:	TC-ART-06-2015-001672.R1
Article Type:	Paper
Date Submitted by the Author:	19-Aug-2015
Complete List of Authors:	Yamaguchi, Shiori; Tokyo Metropolitan University, Department of Applied Chemistry, Graduate School of Urban Environmental Sciences Moriyama, Kenji; Tokyo Metropolitan University, Department of Applied Chemistry, Graduate School of Urban Environmental Sciences Kajihara, Koich; Tokyo Metropolitan University, Department of Applied Chemistry, Graduate School of Urban Environmental Sciences Kanamura, Kiyoshi; Tokyo Metropolitan University, Department of Applied Chemistry, Graduate School of Urban Environmental Sciences; Tokyo metropolitan university,



Journal Name

ARTICLE

Deep-ultraviolet transparent monolithic sol-gel derived silica-REPO₄ (RE = Y, La-Lu except Pm) glass-ceramics: characterization of crystal structure and ultraviolet absorption edge, and application to narrow-band UVB phosphors

Received 00th January 20xx,
Accepted 00th January 20xx

DOI: 10.1039/x0xx00000x

www.rsc.org/

Shiori Yamaguchi, Kenji Moriyama, Koichi Kajihara,* Kiyoshi Kanamura

Monolithic silica glasses containing nanocrystals of rare-earth (RE) orthophosphates (REPO₄, where RE = Y, La-Lu except Pm) were prepared by a cosolvent-free sol-gel method. Despite the large refractive index mismatch between the REPO₄ nanocrystals and the host silica glass, these glasses are highly transparent in the deep-ultraviolet (deep-UV, DUV) spectral region (≤ 300 nm) because the Rayleigh scattering is suppressed by the small crystal size (~ 5 – 10 nm) and narrow size distribution. The encapsulation of the nanocrystals in the silica matrix increases the stability range of the monoclinic monazite form. The UV absorption edge originates from the electronic transition in PO₄ units at RE = Y, La, Gd, and Lu or from the $4f$ – $5d$ or charge transfer transition for other RE³⁺ ions with partially filled $4f$ shells. Glasses containing Gd³⁺ ions exhibit a bright narrow UV photoluminescence (PL) band at ~ 313 nm, and the PL efficiency is significantly increased by the addition of Pr³⁺ ions acting as photosensitizers for Gd³⁺ ions. The absorbance and internal and external quantum efficiencies of the PL band of a glass containing Gd_{0.9}Pr_{0.1}PO₄ nanocrystals under excitation at 230 nm were ~ 0.91 , ~ 0.70 , and ~ 0.63 , respectively. Because of the high quantum efficiency this type of glass is promising as a narrow-band UV phosphor used for UVB (280–320 nm) phototherapy.

Introduction

Rare-earth (RE) ions are useful luminescent centers because of the high efficiency and wavelength variation of their photoemission, and they are usually used with transparent host materials. Silica glass is attractive as a host material for luminescent centers because of its wide transparency window from near infrared (IR) to vacuum-ultraviolet (VUV, ≤ 200 nm) spectral regions, mechanical strength, chemical stability, radiation hardness, and shape workability. In particular, its high transparency in ultraviolet (UV) and deep-ultraviolet (DUV, ≤ 300 nm) spectral regions^{1–3} is suitable for developing glass-based DUV phosphors that cannot be realized by conventional multicomponent glasses of low UV transparency. Although the solubility of RE ions in silica glasses is low, it can be increased by incorporating specific elements. Phosphorus (P) enhances the dissolution of RE ions in silica glasses.^{4–14} However, the dissolution mechanism remained elusive until recently. Formation of RE phosphate nanocrystals⁶ and preferential coordination of P to RE ions^{11,12} have been observed in samples prepared using vapor-phase methods. Clustering of RE ions and P has also been suggested in sol-gel derived RE–P codoped glasses.¹³ These observations indicate a

strong affinity between RE ions and P in silica glasses.

We developed sol-gel techniques to prepare monolithic transparent RE–P codoped glasses¹⁴ and recently evidenced that RE ions are dissolved by forming REPO₄ nanocrystals in glasses prepared at a P:RE molar ratio of 1:1.¹⁵ Although the refractive indices of REPO₄ nanocrystals (~ 1.8 at 633 nm)^{16,17} and the host silica (~ 1.457 at 633 nm)¹⁸ are largely different, optical loss by Rayleigh scattering is insignificant because of the small average crystal size (~ 5 nm). REPO₄ crystallizes into two different forms; the monoclinic form (monazite, space group no. 14, $P2_1/c$) is stable at La–Gd, whereas the tetragonal form (xenotime, space group no. 141, $I4_1/amd$) is stable at Tb–Lu and Y.^{19,20} However, metastable monoclinic TbPO₄ nanocrystals are precipitated in the sol-gel-derived glasses. REPO₄ powders containing Tb³⁺ ions are commercially used as green phosphors in fluorescence lamps, and silica-(Tb,Ce)PO₄ glass-ceramics exhibit bright green photoluminescence (PL) with external quantum efficiencies as large as ~ 0.76 under excitation at 290 nm.

The high DUV transparency of silica-REPO₄ glass-ceramics is suitable for application to UV–DUV phosphors. A recent report has indicated that (La,Gd,Pr)PO₄ powder exhibits intense UV PL at 312 nm originating from the $^6P_{7/2} \rightarrow ^8S_{7/2}$ $4f$ – $4f$ transition of Gd³⁺ ions.²¹ Since this narrow PL band is located in the UVB region (280–320 nm) and does not contain DUV radiation harmful to living organisms, it has attracted attention as “narrow-band UVB emission” in medical and biological

Department of Applied Chemistry, Graduate School of Urban Environmental Sciences, Tokyo Metropolitan University, 1-1 Minami-Osawa, Hachioji, Tokyo 192-0397, Japan. E-mail: kkaji@tmu.ac.jp

fields. This UV PL band is excited via the $4f-5d$ transition of codoped Pr^{3+} ions at $\lesssim 230$ nm, which is much stronger than the $4f-4f$ transitions of Gd^{3+} ions. This photosensitization mechanism is confirmed in various hosts including REPO_4 ,^{21,22} $\text{BaRE}_4\text{Si}_5\text{O}_{17}$,²³ $\text{RE}_3\text{Al}_5\text{O}_{12}$,²⁴ REBO_3 ,^{25,26} $\text{Ca}_3\text{RE}_3(\text{BO}_3)_5$,²⁶ REF_3 ,²⁷ and REAlO_3 ,²⁸ and is useful in increasing the PL quantum efficiency of the UV PL band of Gd^{3+} ions. However, to maintain the high PL efficiency, energy migration among Gd^{3+} ions and subsequent nonradiative transitions at killer centers need to be suppressed by additionally incorporating inert La^{3+} ions. This restricts the maximum fraction of Gd^{3+} ions to ~ 0.35 in $(\text{La,Gd,Pr})\text{PO}_4$ powder.²¹ This problem may be avoided in glass-ceramics containing REPO_4 nanocrystals because the number of RE ions participating in the energy migration process is small. Glass-ceramics containing REPO_4 nanocrystals have also been developed recently from several multicomponent glass systems.²⁹⁻³¹ However, because of the low DUV transparency, their application to UV phosphors may be difficult.

In this paper, we report sol-gel synthesis and characterization of silica- REPO_4 glass-ceramics for RE elements Y and La-Lu except Pm. Variations in the structure of the REPO_4 nanocrystals and the UV absorption edge with substitution of RE ions were examined. The PL spectroscopy of Gd-doped glasses revealed that Gd,Pr-doped glass is an efficient narrow-band UVB phosphor.

Experimental procedure

Glass samples were synthesized by a cosolvent-free sol-gel method, which does not require additives such as alcohols, organic solvents, polymers, and surfactants.^{14,15,32-34} A dilute aqueous solution of nitric acid was added to 25 mmol (5.2 g) of tetraethoxysilane (TEOS, Shin-Etsu Chemical) and stirred for 55 min at 20°C in a sealed plastic container to form a clear solution with a TEOS : H_2O : HNO_3 molar ratio of 1 : x_1 : 0.002. Triphenylphosphine oxide (TPPO, Tokyo Chemical Industry) was added to this solution and dissolved by stirring for another 5 min. The resultant solution was further mixed with an aqueous solution of RE acetates and a Brønsted base, ammonium acetate (AcONH_4 , Wako Chemicals) or imidazole (Wako Chemicals), to form a solution with an overall TEOS : H_2O : HNO_3 : base : TPPO : RE molar ratio of 1 : $x_1 + x_2$: 0.002 : y : 0.01 : 0.01, where $x_1 + x_2 = 10$. After stirring for 1 min, the stirring bar was removed and the solution was maintained at 20°C until gelation. The resultant wet gel was aged for 1 day at 60°C. The container was then opened, the solvent phase was discarded, and the gel was gently dried at 60°C. The dried gel was finally sintered in a tube furnace heated to 1150–1300°C at a rate of 200°C h^{-1} and held there for 0–1 h. The sintering atmosphere was changed from air to helium at 600°C. For the Ce-doped sample a small amount of hydrogen was additionally introduced between 1000 and 1100°C to prevent oxidation of Ce^{3+} ions. For the Eu-doped sample a small amount of oxygen was additionally introduced above 600°C to avoid reduction of Eu^{3+} ions. In addition to the glass samples, powder samples of REPO_4 were synthesized from RE acetates and $\text{NH}_4\text{H}_2\text{PO}_4$

(Kanto Chemical). Their aqueous solutions were mixed while stirring. The mixture was dried at 80°C, crushed, heated to 1200°C in air at a rate of 200°C h^{-1} , and maintained for 5 h at 1200°C. The resultant glasses were characterized by conventional and vacuum-ultraviolet (VUV) spectrometers (U-4100, Hitachi, resolution 1 nm, and VU-201, Bunkou-Keiki/JASCO, resolution 1 nm, respectively), and dispersive visible and Fourier-transform (FT) IR Raman spectrometers (NRS-1000, JASCO, excitation at 532 nm and Model 960, Nicolet, excitation at 1064 nm, respectively). Powder samples were examined by X-ray diffraction (XRD; SmartLab, Rigaku) and transmission electron microscopy (TEM; JEM-3200FS, JEOL, operated at 300 kV). Rietveld analysis and calculation of theoretical XRD patterns were performed using RIETAN-FP.³⁵ The PL spectra of the Gd-doped samples were measured using an integrating sphere (4P-GPS-053-SL, Labsphere) connected to a charge-coupled device (CCD) spectrometer (EPP2000C, StellarNet, resolution 3 nm) and the PL intensity was calibrated using a photodiode power meter (3A-P, OPHIR). Excitation light was derived from a fluorophotometer (F-7000, Hitachi) using an optical fiber.

Results

All precursor solutions were gelled for ~ 30 –120 min after removing the stirring bar, and they yielded macroporous gels as a result of phase separation in parallel with gelation.^{14,32-34} The x_1 and y values were varied at 1.7–2.0 and 0.01–0.02, respectively, to control the pore size in order to obtain densification of the gels at approximately 1200°C. For the synthesis of the Tm-, Yb-, and Lu-doped glasses, imidazole ($\text{p}K_a = 7.0$) was used as the base^{34,36} because of the high acidity of relevant RE^{3+} ions.^{37,38} Ammonium acetate ($\text{p}K_a = 4.8$) was used for other systems. Monolithic transparent glasses, shown in Fig. 1, were obtained in ~ 1 week for all compositions.

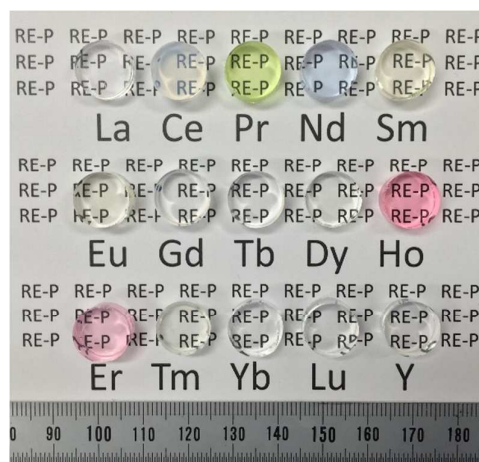


Fig. 1 Photograph of sol-gel-derived silica- REPO_4 glass-ceramics. The diameter and thickness of the glasses are ~ 1 cm and ~ 0.5 cm, respectively.

Fig. 2 shows the powder XRD patterns of the crushed glasses. Weak and broad diffraction peaks were observed, suggesting precipitation of crystals with small particle sizes. The peaks were assigned to monoclinic REPO₄ at La–Tb and tetragonal REPO₄ at Er–Lu and Y. These two phases probably coexisted at Dy. The average diameter of the crystals, D , was evaluated using the Scherrer equation, $D = K\lambda/\beta\cos\theta$, where K is the Scherrer constant ($K = 1$ for β expressed in the integral breadth), λ is the wavelength of the Cu K α X-ray emission line, and θ and β are the diffraction angle and integral breadth, respectively, of the strongest peak [021 ($\sim 28\text{--}29^\circ$) for monoclinic phases and 200 ($\sim 26^\circ$) for tetragonal phases]. The evaluated D values were typically $\sim 5\text{--}10$ nm, whereas the value for the Ce-doped glass was slightly larger (~ 17 nm).

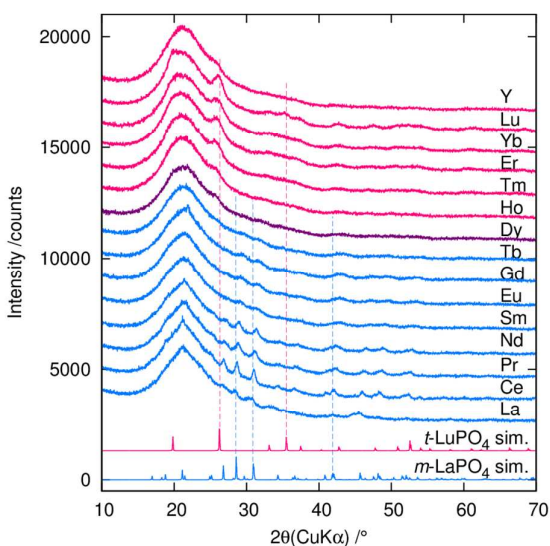


Fig. 2 Powder XRD patterns of crushed glasses. Simulated patterns for monoclinic (*m*-) LaPO₄ and tetragonal (*t*-) LuPO₄ were calculated using structural parameters reported in ref. 19.

Fig. 3 shows the Raman spectra of the glass samples. An FT-Raman spectrometer was mainly used to guarantee the wavenumber accuracy. A dispersive Raman spectrometer was used for measurements of the Ho- and Yb-doped glasses because IR PL interfered with the detection of their Raman signals. In all samples, a Raman band at $\sim 980\text{--}1010$ cm⁻¹, attributed to the symmetric stretching mode (ν_1) of the PO₄ tetrahedra in REPO₄, was clearly seen. This band shifted to higher wavenumbers with an increase in atomic number and decrease in cell volume, consistent with Raman studies on REPO₄ powders and single crystals.³⁹ At $\sim 1050\text{--}1100$ cm⁻¹, the antisymmetric stretching mode (ν_3) of the PO₄ tetrahedra was seen. The variation of the peak position of the ν_3 band with atomic number was discontinuous between Tb and Ho, corroborating the transformation between the monoclinic and tetragonal phases observed by XRD (Fig. 2).

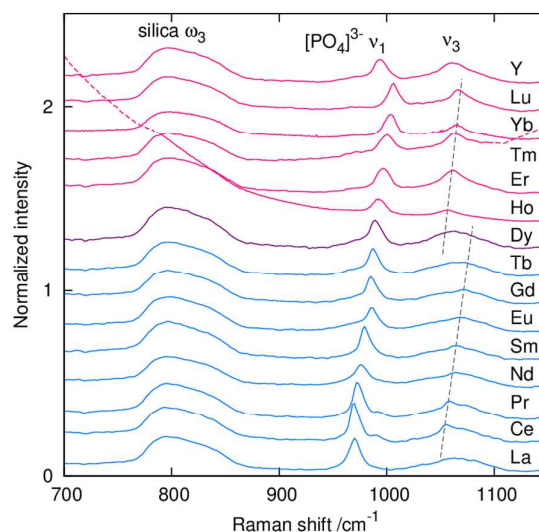


Fig. 3 Raman spectra of glasses shown in Fig. 1.

The La- and Lu-doped glasses, which are the end members of the lanthanoids, and Ce-doped glass, whose D value evaluated from the XRD pattern shown in Fig. 2 was larger than those of other samples, were selected for TEM observations. Fig. 4 shows their TEM images, where dark spots attributable to REPO₄ crystals were observed. Several spots exhibited clear lattice fringes. The average diameters and their relative standard deviations (RSD), respectively, were calculated to be ~ 6.0 nm and $\sim 17\%$ for the La-doped glass, ~ 6.2 nm and $\sim 20\%$ for the Lu-doped glass, and ~ 14 nm and $\sim 39\%$ for the Ce-doped glass. These results were consistent with the D values evaluated by XRD. The distribution of diameters of the REPO₄ nanocrystals was relatively narrow for the La- and Lu-doped glasses, similarly to the results of the Tb-doped glasses reported previously (~ 5.7 nm and $\sim 20\%$).¹⁵

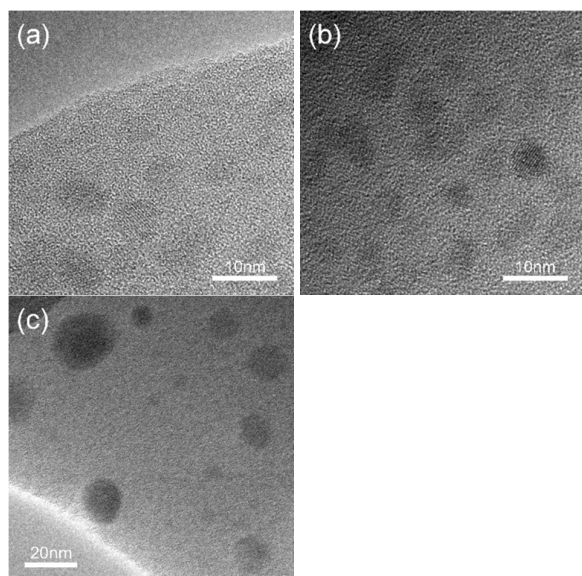


Fig. 4 TEM images of crushed La-doped (a), Lu-doped (b), and Ce-doped (c) glasses.

The optical absorption spectra are shown in Fig. 5a for glasses with RE = La–Gd and in Fig. 5b for those with RE = Tb–Lu and Y. Most of the glasses exhibited good UV transparency despite the presence of REPO₄ nanocrystals with high refractive indices (~1.8^{16,17}). Sharp 4*f*–4*f* transitions of doped RE³⁺ ions were also seen. The position of the UV absorption edges varied significantly from sample to sample, and was located in the VUV spectral region in several samples. Optical loss α due to Rayleigh scattering by REPO₄ nanocrystals with diameter D may be given by

$$\alpha = 4\pi^4 f_v \left(\frac{m^2 - 1}{m^2 + 2} \right)^2 \frac{D^3}{\lambda^4}$$

where f_v is the volume fraction of the REPO₄ phase and m is the ratio of the refractive indices between SiO₂ (1.457 at 633 nm¹⁸) and REPO₄ phases. Because the refractive indices of REPO₄ crystals are less influenced by the differences in RE ions,¹⁷ the m value was approximated to be 1.23 using the refractive index of LaPO₄ ($n_{av} = 1.791$; $n_x = 1.774$, $n_y = 1.770$, and $n_z = 1.828$ at 633 nm¹⁶) on the assumption that the wavelength dependence of m is small. The α values were calculated at $D = 5, 10, 20,$ and 30 nm and are plotted as dashed lines in Figs. 5a and 5b. In most samples, the optical loss was smaller than the curve calculated at $D = 10$ nm, indicating that the Rayleigh scattering from the REPO₄ nanocrystals was insignificant because of the small crystal size. Glasses derived by sol–gel methods often contain a large number of SiOH groups, typically on the order of 10^{20} cm⁻³. The concentration of SiOH groups evaluated from the peak intensity of the first overtone band of the SiO–H stretching mode at ~7270 cm⁻¹ (not shown)¹⁴ was ~2–4 × 10²⁰ cm⁻³.

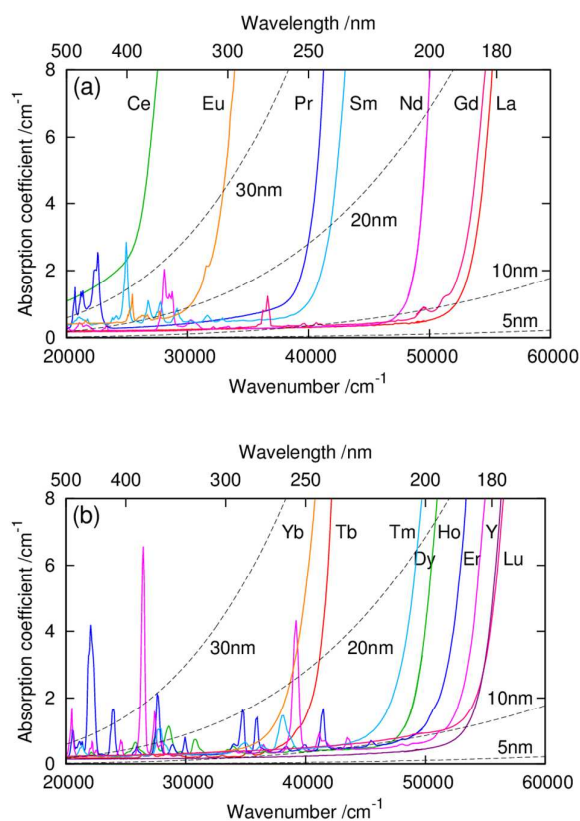


Fig. 5 Optical absorption spectra of glasses shown in Fig. 1 with (a) RE = La–Gd and (b) Tb–Lu and Y.

Fig. 6 plots the energies of the UV absorption edge, defined here as the wavenumber at which the absorption coefficient of the spectra shown in Figs. 5a and 5b becomes 5 cm⁻¹. The energies of the absorption edge of glasses with RE = Y, La, Ga, and Lu, whose 4*f* shells are vacant, half-filled, or completely filled, were larger than those of other glasses. In other samples containing RE³⁺ ions with partially filled 4*f* shells, the absorption edge energy was at a maximum for the Nd- and Er-doped glasses. This tendency was similar to the variation of peak energies of the lowest 4*f*–5*d* and oxygen-to-RE charge transfer (CT) bands observed by PL excitation spectroscopy of LaPO₄ doped with RE³⁺ ions.^{40–42}

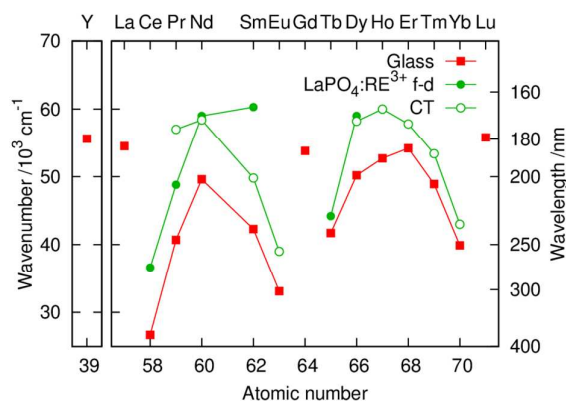


Fig. 6 Energy of UV absorption edge (defined as absorption coefficient = 5 cm^{-1}) of glasses shown in Figs. 5a and 5b (red squares) and peak energies of PL excitation spectra for LaPO_4 microcrystals doped with various RE^{3+} ions at 2 at% (green circles) taken from ref. 40. The origin of the peaks are assigned to the $4f-5d$ (filled circles) or charge transfer (CT, open circles) transitions of doped RE^{3+} ions.

The UV PL from Gd^{3+} ions was measured for Gd-doped glasses and REPO_4 powders containing Gd^{3+} ions. In addition to the Gd-doped glass shown in Fig. 1, a Gd,Pr-doped glass was prepared at a Gd:Pr molar ratio of 9:1 while maintaining the total number of RE ions. Fig. 7 shows a photograph and optical absorption spectra of these glasses and the Pr-doped glass shown in Fig. 1. In the Gd- and Gd,Pr-doped glasses, sharp peaks attributed to the $4f-4f$ transitions of Gd^{3+} ions were seen. The absorption edges of the Pr- and Gd,Pr-doped glasses originated from the $4f-5d$ transition of Pr^{3+} ions,^{21,22,40,41} and the apparent high-energy shift for the Gd,Pr-doped glass was due to the small concentration of Pr^{3+} ions (one-tenth that of the Pr-doped glass).

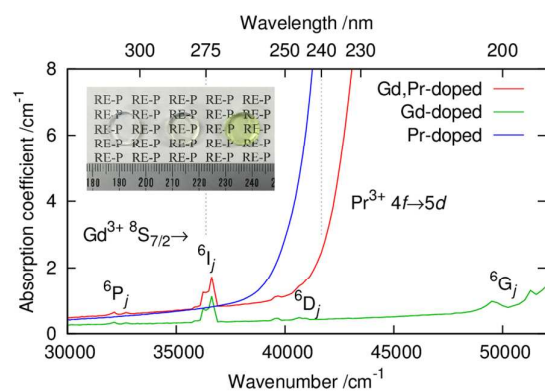


Fig. 7 Optical absorption spectra of Gd,Pr-, Gd-, and Pr-doped glasses. A photograph of the Gd-, Gd,Pr-, and Pr-doped glasses (left to right) is also shown. The spectra of the Gd- and Pr-doped glasses are identical to those shown in Fig. 5. In the Gd,Pr-doped glass, the Gd:Pr molar ratio was 9:1 and total RE concentration was the same as those of the other two glasses.

The REPO_4 powders were synthesized at RE compositions identical to that of the glass samples (GdPO_4 and $\text{Gd}_{0.9}\text{Pr}_{0.1}\text{PO}_4$) and the composition at which the UV PL intensity reaches its maximum under excitation at 172 nm ($\text{Gd}_{0.35}\text{Pr}_{0.05}\text{La}_{0.60}\text{PO}_4$).²¹ Fig. 8 shows XRD patterns and Rietveld analyses of the powder samples. Single-phase monoclinic samples were obtained at all compositions; in each sample the fraction of the tetragonal phase was less than 1% and other impurity phases were not observed. Lattice expansion accompanied by the incorporation of Pr^{3+} and La^{3+} ions was clearly seen.

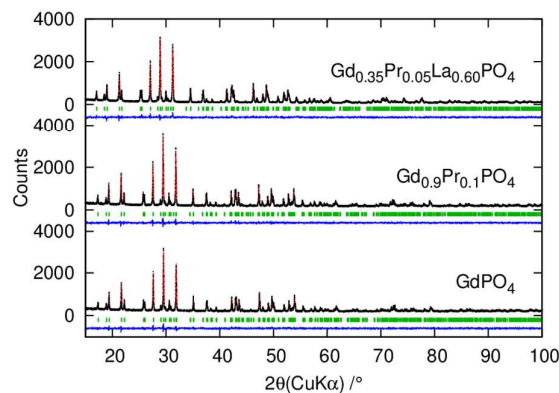


Fig. 8 XRD patterns and Rietveld analyses of GdPO_4 , $\text{Gd}_{0.9}\text{Pr}_{0.1}\text{PO}_4$, and $\text{Gd}_{0.35}\text{Pr}_{0.05}\text{La}_{0.60}\text{PO}_4$ powders. Space group no. 14, $P2_1/c$. GdPO_4 : $a = 6.3367(2) \text{ \AA}$, $b = 6.8440(10) \text{ \AA}$, $c = 8.0012(3) \text{ \AA}$, $\beta = 126.219(2)^\circ$, $R_{\text{wp}} = 6.08\%$, $R_l = 3.90\%$, $R_f = 2.91\%$, $S = 1.01$. $\text{Gd}_{0.9}\text{Pr}_{0.1}\text{PO}_4$: $a = 6.3473(2) \text{ \AA}$, $b = 6.8583(10) \text{ \AA}$, $c = 8.0182(2) \text{ \AA}$, $\beta = 126.240(2)^\circ$, $R_{\text{wp}} = 6.29\%$, $R_l = 3.60\%$, $R_f = 2.40\%$, $S = 1.03$. $\text{Gd}_{0.35}\text{Pr}_{0.05}\text{La}_{0.60}\text{PO}_4$: $a = 6.4522(2) \text{ \AA}$, $b = 6.9907(12) \text{ \AA}$, $c = 8.1855(3) \text{ \AA}$, $\beta = 126.453(2)^\circ$, $R_{\text{wp}} = 8.18\%$, $R_l = 4.24\%$, $R_f = 1.95\%$, $S = 1.08$. In each sample the fractional coordinates were fixed at the values of GdPO_4 reported in ref. 19.

Fig. 9 shows the PL spectra of the Gd,Pr- and Gd-doped glasses and the REPO_4 powders taken under excitation with the $^8\text{S}_{7/2} \rightarrow ^6\text{I}_7$ transition of Gd^{3+} ions at 275 nm and the $4f-5d$ transition of Pr^{3+} ions at 240 or 230 nm. A PL band due to the $^6\text{P}_{7/2} \rightarrow ^8\text{S}_{7/2}$ transition of Gd^{3+} ions was observed at $\sim 313 \text{ nm}$. The peak position was shifted to longer wavelengths compared with that of the powder samples ($\sim 312 \text{ nm}$). The area for this PL band, shown in Fig. 9, is equal to the number of emitted photons, N_{em} . The areas for the excitation bands in the spectrum of an empty sphere and a sample spectrum correspond to the number of excitation photons in the empty sphere, N_{ex}^0 , and the number not absorbed by the sample, N_{ex} , respectively. From these values, the absorbance and internal and external quantum efficiencies were calculated as $\text{Abs.} = (N_{\text{ex}}^0 - N_{\text{ex}}) / N_{\text{ex}}^0$, $\text{IQE} = N_{\text{em}} / (N_{\text{ex}}^0 - N_{\text{ex}})$, and $\text{EQE} = \text{Abs.} \times \text{IQE} = N_{\text{em}} / N_{\text{ex}}^0$, respectively, and the results are listed in Table 1.

Table 1 Values of absorbance and internal and external quantum efficiencies (IQE and EQE, respectively) evaluated from PL spectra shown in Fig. 9.

Excitation (nm)		Glass		Powder		
		Gd,Pr-doped	Gd-doped	GdPO ₄	Gd _{0.9} Pr _{0.1} PO ₄	Gd _{0.35} Pr _{0.05} La _{0.60} PO ₄
275	Abs. ^(a)	0.34	0.32	0.14	0.12	0.06
	IQE	0.39	0.46	0.10	0.15	0.7
	EQE ^(a)	0.13	0.15	0.01	0.02	0.04
240	Abs. ^(a)	0.65	0.23	0.02	0.02	0.01
	IQE	0.53	0.09	(c)	(c)	(c)
	EQE ^(a)	0.34	0.02	(b)	(b)	0.01
230	Abs. ^(a)	0.91	0.23	0.01	0.03	0.04
	IQE	0.70	0.02	(c)	0.4	0.7
	EQE ^(a)	0.63	0.01	(b)	0.01	0.03

^(a) Uncertainties: ± 0.02 .

^(b) Below the limit of quantification (<0.01).

^(c) Uncertainties: ± 0.5 or more.

Under excitation at 275 nm, values recorded for the Gd,Pr- and Gd-doped glasses were similar. At 240 and 230 nm, in contrast, the values for the Gd,Pr-codoped glass were much better than those for the Gd-doped glass. In the Gd,Pr-doped glass, measurements at 230 nm, which gave better values than measurements at 240 nm, yielded IQE and EQE values of ~ 0.70 and ~ 0.63 , respectively. Measurements at shorter wavelengths were not possible because of the absence of sensitivity of the CCD spectrometer below ~ 220 nm. Values recorded for the powder samples were worse than the glasses at all excitation wavelengths, except that the IQE values of the Gd_{0.35}Pr_{0.05}La_{0.60}PO₄ powder were relatively large (~ 0.7). The small PL intensity of the powder samples was originated mainly from the weak absorption; the absorption was stronger at 275 nm than at 230 and 240 nm and insensitive to the presence of Pr³⁺ ions. In the Pr-doped glass and powder samples visible and UV PL bands attributed to transitions from the 5d, ³P_j, and ¹D_j levels of Pr³⁺ ions^{22,24} were not observed.

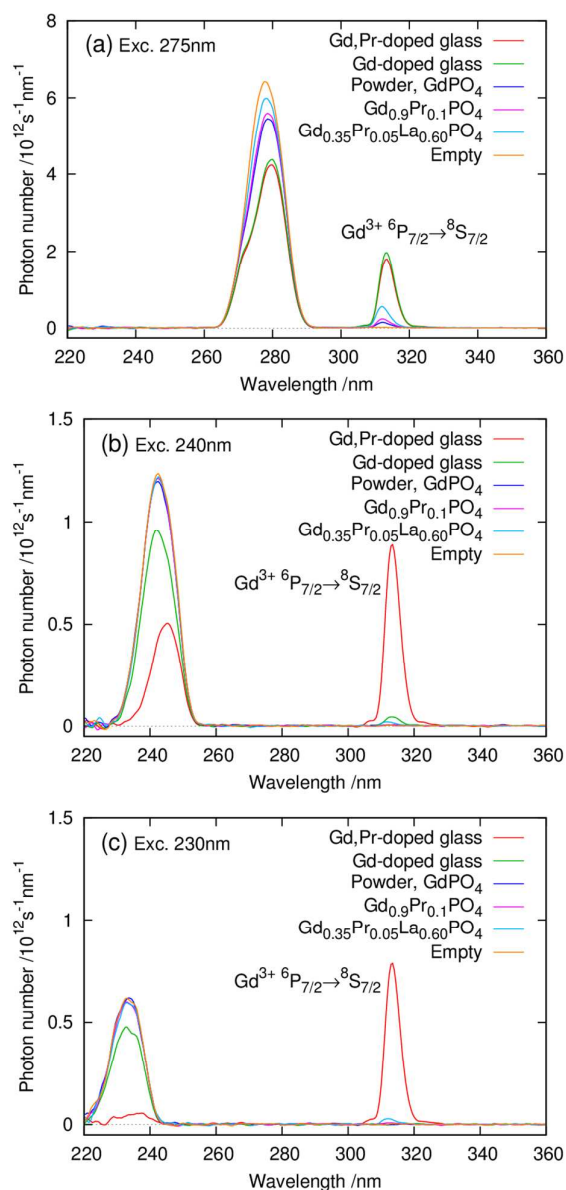


Fig. 9 PL spectra of Gd,Pr- and Gd-doped glasses and powder samples of GdPO_4 , $\text{Gd}_{0.9}\text{Pr}_{0.1}\text{PO}_4$, and $\text{Gd}_{0.35}\text{Pr}_{0.05}\text{La}_{0.60}\text{PO}_4$ measured under excitation at (a) 275 nm, (b) 240 nm, and (c) 230 nm.

Discussion

The transition between monoclinic and tetragonal phases of REPO_4 usually takes place between GdPO_4 and TbPO_4 .^{19,20} However, for samples prepared by wet-chemical methods below 1000°C, monoclinic phases can be obtained for TbPO_4 , DyPO_4 , and HoPO_4 ,²⁰ probably because the low synthesis temperature stabilizes phases with lower symmetries. These metastable monoclinic phases are usually transformed to stable tetragonal phases after heating above 1000°C.²⁰ In the glasses prepared in this study, however, the monoclinic phase was stabilized at Tb and two phases coexisted at Dy, despite

the fact that they were sintered at 1200°C. Thus, the monoclinic phase is probably more stable in REPO_4 nanocrystals formed in the sol-gel-derived glasses than in bulk REPO_4 samples. Encapsulation by the silica matrix may be responsible for this phenomenon because a simple reduction of particle size usually leads to transformation to phases with higher symmetries. The monoclinic phase may be more suitable for optical applications because the site symmetry of a RE ion in the monoclinic phase (1) is lower than that in the tetragonal phase ($\bar{4}m2$) and the probabilities of the $4f-4f$ transitions would be larger in the former host.

As shown in Figs. 2 and 3, all glasses prepared in this study contained REPO_4 nanocrystals, whose refractive indices (~ 1.8) are much larger than that of silica glass ($\sim 1.4-1.5$). However, Rayleigh scattering in the DUV spectral region was significantly small in most of the glasses, making it possible to analyze the origin of the UV absorption edge. Several glasses were even transparent in the VUV spectral region below ~ 200 nm. This is evidently due to the small average diameter of REPO_4 nanocrystals ($\sim 5-10$ nm) and the narrow size distribution. However, transparency of the Ce-doped glass was not good because of an increase in the size of the CePO_4 nanocrystals (Fig. 4). The poor transparency might be because of the hydrogen treatment during sintering to suppress the oxidation of Ce^{3+} ions, and the transparency would be improved by modifying the synthesis procedure.

As shown in Fig. 6, the variation of energy of the UV absorption edge with atomic number of RE^{3+} ions exhibits two maxima at 60 (Nd) and 68 (Er). The observed dependence of the absorption edge energy on the atomic number is similar to the variation of the peak energies of the lowest $4f-5d$ and CT bands of RE-doped LaPO_4 ,⁴⁰ indicating that their origins are the same. The peak energy is systematically larger than the absorption edge energy simply because the absorption edge corresponds to the low-energy tail of the absorption band. Thus, the UV absorption edge of glasses doped with RE^{3+} ions with partially filled $4f$ shells (except Gd) is determined by the $4f-5d$ or CT absorption of RE^{3+} ions. In the Y-, La-, Gd-, and Lu-doped glasses, in contrast, the $4f-5d$ and CT transitions are absent or shifted to higher energies; in this case, the UV absorption edge is attributable to the transition in PO_4 units. The absorption edge energy of the transition in PO_4 units is reported to be smaller for the monoclinic REPO_4 than for the tetragonal REPO_4 ,⁴³ probably because of the lower symmetry of the PO_4 site in the monoclinic form. Indeed, the observed absorption edge energy of the La- and Gd-doped glasses is slightly smaller than that of the Lu- and Y-doped glasses.

The UV PL band of Gd^{3+} ions at ~ 313 nm originating from the ${}^6\text{P}_{7/2} \rightarrow {}^8\text{S}_{7/2}$ transition can be excited via the ${}^8\text{S}_{7/2} \rightarrow {}^6\text{I}_j$ transition at ~ 275 nm. The absorbance at 275 nm is larger for the glasses than for the powder samples, although the average concentration of Gd^{3+} ions in the glasses ($\sim 2 \times 10^{20} \text{ cm}^{-3}$) is two orders of magnitude smaller than that of the GdPO_4 powder ($\sim 1.4 \times 10^{22} \text{ cm}^{-3}$). The smaller absorbance in the powders is probably due to the high refractive index and the resultant significant surface reflection. Indeed, the absorbance of the GdPO_4 powder decreases with a decrease in wavelength (Table

1) and simultaneous increase in the refractive index. Similar tendency is observed for the $\text{Gd}_{0.9}\text{Pr}_{0.1}\text{PO}_4$, and $\text{Gd}_{0.35}\text{Pr}_{0.05}\text{La}_{0.60}\text{PO}_4$ powders, although their absorbance at 230 nm is much larger than that at 275 nm. In glasses, in contrast, light scattering inside the glass is largely suppressed and excitation light penetrates through the whole thickness homogeneously. This mechanism facilitates the absorption of excitation light by REPO_4 nanocrystals in the glasses.

Under excitation at 275 nm, the IQE values of the Gd- and Gd,Pr-doped glasses are comparable at ~ 0.4 . However, the IQE values of the GdPO_4 and $\text{Gd}_{0.9}\text{Pr}_{0.1}\text{PO}_4$ powders are evidently smaller (~ 0.10 – 0.15). This difference is probably explained by considering the size of the GdPO_4 crystals. The critical distance for energy transfer between Gd^{3+} ions appears to be 0.5–0.6 nm.^{44,45} The Gd–Gd distance in GdPO_4 is ~ 0.40 – 0.42 nm, which is small enough to cause a rapid migration of excitation energy among Gd^{3+} ions. Although the rate of energy transfer in GdPO_4 is not available, a detailed study has been made for LiGdF_4 , whose Gd–Gd distance is ~ 0.38 nm.⁴⁶ The average number of steps and the diffusion length in the energy migration process among the Gd^{3+} ions in LiGdF_4 at 298K are $\sim 3.1 \times 10^4$ and ~ 66 nm, respectively. The average diffusion length is much larger than the average diameter of GdPO_4 nanocrystals in the Gd-doped glasses (~ 5 – 10 nm). Thus, the energy migration in the GdPO_4 nanocrystals is probably considerably restricted, resulting in a suppression of concentration quenching, i.e., a deactivation of the excitation energy at killer centers. This mechanism explains the high IQE values of the glasses, even without the dilution of Gd^{3+} ions with inert (e.g. La^{3+} and Y^{3+}) ions, which is commonly required for many Gd-based UV phosphors. This mechanism is also consistent with the observation that the IQE value of the $\text{Gd}_{0.35}\text{Pr}_{0.05}\text{La}_{0.60}\text{PO}_4$ powder (~ 0.7) is larger than those of the GdPO_4 and $\text{Gd}_{0.9}\text{Pr}_{0.1}\text{PO}_4$ powders.

The peak wavelength of the UV PL band in the Gd- and Gd,Pr-doped glasses is larger by ~ 1 nm than that in the REPO_4 powder samples. It is not due to the crystal structure because the lattice parameters are nearly equal between the powder and glass-ceramic samples and the peak position is insensitive to the changes in lattice parameters in the powder samples. The low energy shift of the UV PL band in the glasses may be explained by emission from perturbed Gd^{3+} ions (or Gd^{3+} traps), whose peak wavelength is larger than that of emission from regular (unperturbed) Gd^{3+} ions.^{47,48} However, PL attributable to the Gd^{3+} traps is usually weak at room temperature and the exact mechanism remains uncertain.

In REPO_4 , Pr^{3+} ions can be efficient sensitizers for the UV PL band of Gd^{3+} ions probably because PL from the lowest 5d level of Pr^{3+} ions and the ${}^8\text{S}_{7/2} \rightarrow {}^6\text{I}_j$ absorption of Gd^{3+} ions overlap well and the RE–RE distance is small.^{21,24–26} In addition, PL bands attributed to transitions from the 5d and low-lying 4f levels of Pr^{3+} ions were not observed. Thus, the IQE and EQE values are significantly improved by incorporating Pr^{3+} ions and exciting their 4f–5d transition at or below ~ 240 nm. The 4f–5d transition effectively absorbs the excitation light and increases absorbance. The increase in IQE indicates an efficient energy transfer from Pr^{3+} to Gd^{3+} ions, which originates from the

spatial confinement of these ions in REPO_4 nanocrystals and relatively large acceptor-to-donor ratio in the Gd,Pr-doped glass. Thus, incorporation of Pr^{3+} ions significantly increases EQE, which is given by the product of absorbance and IQE. In addition, these values are better for excitation at 230 nm than that at 240 nm. These values are probably improved at shorter wavelengths, where the absorption due to the 4f–5d transition becomes more intense, and by optimizing the ratio between Gd^{3+} and Pr^{3+} ions.

It is noteworthy that the IQE value of the Gd,Pr-doped glass is high, despite the relatively high concentration of SiOH groups ($\sim 10^{20}$ cm^{-3}). This observation suggests that the phonon energy of the SiO–H stretching mode (~ 3700 cm^{-1}) is no longer large enough to enhance the nonradiative transition from the ${}^6\text{P}_{7/2}$ level of Gd^{3+} ions.

Conclusions

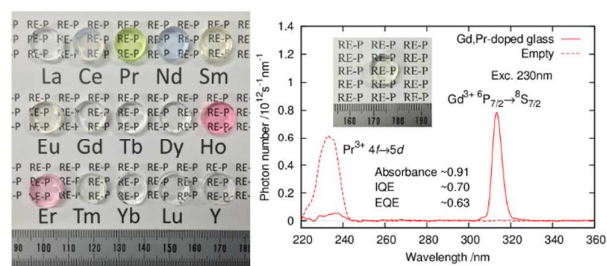
Silica glasses containing REPO_4 nanocrystals (RE = Y, La–Lu except Pm) while highly transparent in the deep-ultraviolet (deep-UV, DUV) spectral region were prepared by a cosolvent-free sol–gel method without using additives such as alcohols, organic solvents, and polymers. The small average crystal size and narrow size distribution suppress Rayleigh scattering despite the large refractive index mismatch between the REPO_4 nanocrystals and silica glass. In these glasses, the stability of monoclinic REPO_4 increases and a transition between monoclinic and tetragonal phases is observed for DyPO_4 . The UV absorption edge is determined by the electronic transition in PO_4 units for glasses containing Y, La, Gd, and Lu, and by the 4f–5d or charge transfer transition for glasses containing other RE^{3+} ions with partially filled 4f shells. The UV photoluminescence (PL) originating from the ${}^6\text{P}_{7/2} \rightarrow {}^8\text{S}_{7/2}$ transition of Gd^{3+} ions is stronger in Gd-doped glasses than in REPO_4 powder samples containing Gd^{3+} ions. This is partly because of the small crystal size, which restricts the number of Gd^{3+} ions participating in the energy migration process and suppresses the concentration quenching. In addition, the absorption of excitation light is significantly enhanced by the reduction of light scattering at the interface between the REPO_4 nanocrystals and the silica host. It is noteworthy that the absorbance of the glasses is much larger than that of the REPO_4 powders, resulting in a high external quantum efficiency. The PL quantum efficiency is improved by incorporating Pr^{3+} ions and utilizing the energy transfer to Gd^{3+} ions. The energy transfer is most likely facilitated by the spatial confinement of Gd^{3+} and Pr^{3+} ions in REPO_4 nanocrystals, which cannot be realized by simple codoping of these ions in transparent host materials. The values of absorbance and internal and external quantum efficiencies recorded for a Gd,Pr-codoped glass under excitation at 230 nm were ~ 0.91 , ~ 0.70 , and ~ 0.63 , respectively, and these values are probably increased at shorter wavelengths where the absorption by Pr^{3+} ions is stronger and by optimizing the RE composition of the nanocrystals.

Acknowledgements

We wish to thank Mr. Eiichi Watanabe of Tokyo Metropolitan University for assistance with TEM observations. This work was partly supported by a Grant-in-Aid for Scientific Research (B) (no. 24350109) from the Japan Society for the Promotion of Science (JSPS).

References

- G. Pacchioni, L. Skuja and D. L. Griscom, Eds. *Defects in SiO₂ and Related Dielectrics: Science and Technology*. Kluwer Academic Publishers, Dordrecht, Netherlands, 2000.
- D. L. Griscom, *J. Ceram. Soc. Jpn.*, 1991, **99**, 923–942.
- L. Skuja, H. Hosono, M. Hirano and K. Kajihara, *Proc. SPIE*, 2003, **5122**, 1–14.
- K. Arai, H. Namikawa, K. Kumata, T. Honda, Y. Ishii and T. Handa, *J. Appl. Phys.*, 1986, **59**, 3430–3436.
- Y. Ishii, K. Arai, H. Namikawa, M. Tanaka, A. Negishi, T. Handa, *J. Am. Ceram. Soc.*, 1987, **70**, 72–77.
- B. J. Ainslie, S. P. Craig, S. T. Davey, D. J. Barber, J. R. Taylor and A. S. L. Gomes, *J. Mater. Sci. Lett.*, 1987, **6**, 1361–1363.
- B. J. Ainslie, S. P. Craig, S. T. Davey and B. Wakefield, *Mater. Lett.*, 1988, **6**, 139–144.
- K. Hattori, T. Kitagawa, K. Shuto, M. Oguma and Y. Ohmori, *Mater. Sci. Eng. B*, 1998, **54**, 15–17.
- M. Nogami, T. Nagakura, T. Hayakawa, and T. Sakai, *Chem. Mater.*, 1998, **10**, 3991–3995.
- C. Canevali, M. Mattoni, F. Morazzoni, R. Scotti, M. Casu, A. Musinu, R. Krsmanovic, S. Polizzi, A. Speghini and M. Bettinelli, *J. Am. Chem. Soc.*, 2005, **127**, 14681–14691.
- A. Saitoh, S. Murata, S. Matsuishi, M. Oto, T. Miura, M. Hirano and H. Hosono, *Chem. Lett.*, 2005, **34**, 1116–1117.
- A. Saitoh, S. Matsuishi, C. Se-Weon, J. Nishii, M. Oto, H. Hirano and H. Hosono, *J. Phys. Chem. B*, 2006, **110**, 7617–7620.
- N. N. Khimich, G. M. Berdichevskii, E. N. Poddenezhnyi, V. V. Golubkov, A. A. Boiko, V. M. Ken'ko, O. B. Evreinov and L. A. Koptelov, *Glass Phys. Chem.*, 2007, **33**, 152–155.
- K. Kajihara, S. Kuwatani and K. Kanamura, *Appl. Phys. Express*, 2012, **5**, 012601.
- K. Kajihara, S. Yamaguchi, K. Kaneko and K. Kanamura, *RSC Adv.*, 2014, **4**, 26692–26696.
- M. J. Weber, *Handbook of Optical Materials*. CRC Press, Boca Raton, 2003.
- G. E. Jellison, Jr., L. A. Boatner and C. Chen, *Opt. Mater.*, 2000, **15**, 103–109.
- I. H. Malitson, *J. Opt. Soc. Am.*, 1965, **55**, 1205–1209.
- Y. Ni, J. M. Hughes and A. N. Mariano, *Am. Mineral.*, 1995, **80**, 21–26.
- U. Kolitsch and D. Holtstam, *Eur. J. Mineral.*, 2004, **16**, 117–126.
- S. Okamoto, R. Uchino, K. Kobayashi and H. Yamamoto, *J. Appl. Phys.*, 2009, **106**, 013522.
- Y. Sato, T. Kumagai, S. Okamoto, H. Yamamoto and T. Kunimoto, *Jpn. J. Appl. Phys.*, 2004, **43**, 3456–3460.
- J. Th. W. de Hair, *J. Solid State Chem.*, 1980, **33**, 33–36.
- A. J. de Vries and G. Blasse, *Mater. Res. Bull.*, 1986, **21**, 683–694.
- A. M. Srivastava, M. T. Sobieraj, S. K. Ruan and E. Banks, *Mater. Res. Bull.*, 1986, **21**, 1455–1463.
- A. J. de Vries, G. Blasse and R. J. Pet, *Mater. Res. Bull.*, 1987, **22**, 1141–1150.
- T. Hirai, H. Yoshida, S. Sakuragi, S. Hashimoto and N. Ohno, *Jpn. J. Appl. Phys.*, 2007, **46**, 660–663.
- Y. Shimizu, Y. Takano and K. Ueda, *J. Lumin.*, 2013, **141**, 44–47.
- X. Yu, F. Song, W. Wang, L. Luo, L. Han, Z. Cheng, T. Sun, J. Tian and E. Y. B. Pun, *J. Appl. Phys.*, 2008, **104**, 113105.
- H. Guo, F. Li, J. Li and H. Zhang, *J. Am. Ceram. Soc.*, 2011, **94**, 1651–1653.
- F. Hu, X. Wei, S. Jiang, S. Huang, Y. Qin, Y. Chen, C.-K. Duan and M. Yin, *J. Am. Ceram. Soc.*, 2015, **98**, 464–468.
- K. Kajihara, M. Hirano and Hosono, *Chem. Commun.*, 2009, **2009**, 2580–2582.
- K. Kajihara, S. Kuwatani, R. Maehana and K. Kanamura, *Bull. Chem. Soc. Jpn.*, 2009, **82**, 1470–1476.
- K. Kajihara, *J. Asian Ceram. Soc.*, 2013, **1**, 121–133.
- F. Izumi and K. Momma, *Solid State Phenom.*, 2007, **130**, 15–20.
- S. Kuwatani, R. Maehana, K. Kajihara and K. Kanamura, *Chem. Lett.*, 2010, **39**, 712–713.
- T. Moeller and H. E. Kremers, *Chem. Rev.*, 1945, **37**, 97–159.
- Y. Suzuki, T. Nagayama, M. Sekine, A. Mizuno and K. Yamaguchi, *J. Less-Common Met.*, 1986, **126**, 351–356.
- G. M. Begun, G. W. Beall, L. A. Boatner and W. J. Gregor, *J. Raman Spectrosc.*, 1981, **11**, 273–278.
- E. Nakazawa and F. Shiga, *Jpn. J. Appl. Phys.*, 2003, **42**, 1642–1647.
- L. van Pieterse, M. F. Reid, R. T. Wegh, S. Soverna and A. Meijerink, *Phys. Rev. B*, 2002, **65**, 045113.
- L. van Pieterse, M. F. Reid, G. W. Burdick and A. Meijerink, *Phys. Rev. B*, 2002, **65**, 045114.
- E. Nakazawa and F. Shiga, *J. Lumin.*, 1977, **15**, 255–259.
- G. Blasse, *Prog. Solid State Chem.*, 1988, **18**, 79–171.
- A. J. de Vries, H. S. Kiliaan and G. Blasse, *J. Solid State Chem.*, 1986, **65**, 190–198.
- A. J. D. Vries, M. F. Hazenkamp and G. Blasse, *J. Lumin.*, 1988, **42**, 275–282.
- C. T. Garapon, B. Jacquier, J. P. Chaminade and C. Fouassier, *J. Lumin.*, 1985, **34**, 211–222.
- A. J. de Vries and G. Blasse, *J. Phys. Colloq.*, 1985, **46**, C7-109–C7-112.



Various silica-REPO₄ glass-ceramics highly transparent in the deep-ultraviolet (DUV, ≤ 300 nm) spectral region (left) and a silica-(Gd,Pr)PO₄ phosphor promising as a narrow-band ultraviolet B (UVB, 280–320 nm) phosphor (right) have been developed by a cosolvent-free sol-gel method.